Tailoring Local Conjugation in Heptazine-Based Polymers through Donor Unit Engineering for Photocatalytic Water Splitting

Xinyu Zhao[a], Wenjing Nie[a], Chunbo Liu[*, a], Yingnan Zhao[b], Renquan Guan[c], Zhao Zhao[*, b], Wenbo Wang[a], Huaqiao Tan[*, b]

[a] *College of Engineering, Jilin Normal University, Siping, 136000, China*

[b] *Key Laboratory of Polyoxometalate and Reticular Material Chemistry of Ministry of Education, Faculty of Chemistry Northeast Normal University, Changchun 130024, China*

[c] *State Key Laboratory of Semiconductor Physics and Chip Technologies, Institute of Semiconductors, Chinese Academy of Sciences, Beijing 100083, China.*

Experimental

Preparation of UC monomer

1.68 g of cyclohexanone and 3.6 g of urea were added to 150 ml of acetic acid solution and refluxed under Ar atmosphere for 10 hours. After the reaction, it was cooled to room temperature and quenched by adding 150 ml of water. The product was extracted by 150 mL of ethyl acetate (150 mL×3). The monomer was taken out of the liquid in rotary evaporator and then dried under vacuum at 60°C.

Characterizations

Transmission electron microscopy (TEM) images and high-resolution transmission electron microscopy (HRTEM) images were carried out on a JEM-2100F microscope at an acceleration voltage of 200 kV. The scanning electron microscope (SEM) images were acquired on a JEOL JSM 4800F SEM. The X-ray diffraction (XRD) patterns were gathered on a Bruker AXS D8 Focus with filtered Cu Kα radiation (λ= 1.54056 Å). Fourier transform infrared (FTIR) spectra were achieved using a Nicolet iS10 FTIR spectrometer. C and N contents were tested by a Vario EL elemental analyzer. The UV-Vis diffuse reflectance spectra (DRS) were collected via a UV-2600 UV-Vis Spectrophotometer (Shimadzu) with $BaSO_4$ as a reference. X-ray photoelectron spectroscopy (XPS) was record on an ESCALABMKII spectrometer with an Al-Kα achromatic X-ray source. N_2 adsorption-desorption isotherms were tested at 77 K using a Quantachrome Autosorb iQ apparatus. Prior to the experiments, the samples were degassed under vacuum at 200 ^oC for 12 h. Photoluminescence (PL) spectra and transient PL lifetime were investigated on a spectrometer (Horiba Jobin Yvon Fluorolog-3) with a QY2 accessory and a time-correlated single-photon counting lifetime spectroscopy system. The ^{13}C NMR spectra and ^2H were performed by Brüker Advance 500. Atomic force microscopy (AFM) study was carried out using Shimadzu SPM-960. The electron paramagnetic resonance (EPR) measurements were carried out on a JEOL JES-FA200 spectrometer. Raman spectroscopic measurements were performed using a 325 nm excitation laser and a wavenumber range 200–2000 $cm^{-1.}$

Electrochemical Analysis

Electrochemical measurements were conducted with a CHI660E Electrochemical Workstation in a standard three-electrode cell using a Pt plate, Ag/AgCl electrode and sample deposited fluoride-tin oxide (FTO) as the counter electrode, reference electrode and working electrode, respectively. The electrolyte solution is 0.2 M Na_2SO_4 aqueous solution. Working electrode manufacturing method is as follows: The 30 mg catalyst is dispersed in 3 ml of ethanol, and then a homogeneous solution is formed by ultrasound. Transfering suspensions onto a 1×4 cm^2 FTO conductive glass using a spin-coating method. The exposure area of the catalyst is 3 cm^2. Finally, the working electrode is obtained by drying at room temperature. For photocurrent measurement (*i-t* curves), a 300 W (CELHXF300, AULIGHT) Xe lamp was used as the light source. The working electrode is irradiated from the back (FTO substrate) to reduce the effect of the experiments. For electrochemical impedance spectroscopy (EIS) experiments, the frequency range is from 0.01 Hz to 10 kHz at -0.2 V.

The apparent quantum yield

The apparent quantum yield (AQY) for H_2 evolution was analysed using the 420, 450, 500, 550 and 600 nm band-pass filter. The average intensity of irradiation was measured by a Coherent Fieldax-TO spectroradiometer. The AQE was calculated based on the following equation:

$$\text{AQE}=\frac{Ne}{Np}\times 100\%=\frac{2\times M\times NA\times h\times c}{S\times P\times t\times \lambda}\times 100\%$$

where Ne is the number of reaction electrons, Np is the incident photons, M is the amount of H_2 molecule, N_A is Avogadro constant, h is the Planck constant, c is the speed of light, S is the irradiation area, P is the intensity of the irradiation, t is the photoreaction time, and λ is the wavelength of the monochromatic light.

Photocatalytic oxidation of methyl phenyl sulphide

10 mg of photocatalyst was added to a 20 mL closed quartz tube containing 0.1 mmol of methyl phenyl sulfide, 1 mL of methanol and 4 mL of acetonitrile and ultrasonically dispersed. The quartz tubes are placed on a parallel reactor with a light source, circulating water cooling and stirrer. The light source is 10 W LED, the reaction temperature is 20 °C and the reaction atmosphere is oxygen. After a certain time of

reaction, the supernatant was collected by centrifugation, and then filtered with a 0.22-micron nylon filter. Finally, the product in the supernatant was detected by chromatography (GC-Agilent 7820).

Calculation methods

First-principle DFT calculations were performed using the plane-wave basis of the projected augmented wave (PAW)[1,2] with exchange-correlation interactions modelled by GGA-PBE[3] functional, as implemented in the Vienna ab initio simulations package (VASP)[4,5]. The DFT + D3 method with the Grimme van der Waals (vdW) correction[6] was employed. Unit cell (1 × 1) was repeated periodically on the x-y plane, a vacuum region of 15 Å was applied along the z-direction, which is enough to avoid the spurious interactions between repeating slabs. The k-space samplings were set as 7 × 7 × 1 for the geometry optimization. Cutoff energy, convergence tolerance of energy and force were set to 500 eV, 10^{-5} eV and 0.02 eV/Å respectively. Then the optimized structures were used to calculate the electronic structures. For calculating the band structures and density of states (DOS), Heyd–Scuseria–Ernzerhof (HSE06) hybrid functional[7] was adopted. The K-point mesh of 3 × 3 × 1 was used for the single point self-consistent calculations.

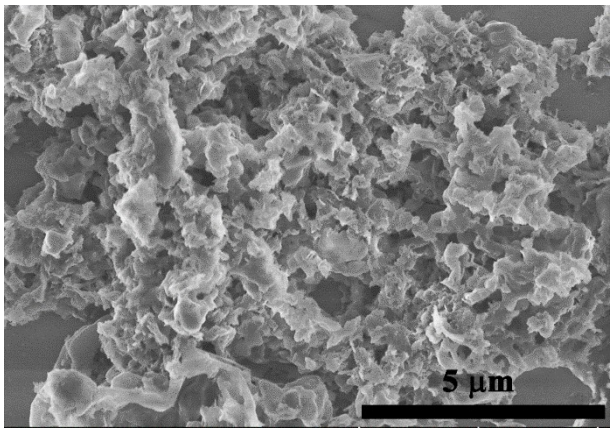

Figure S1. SEM images of g-C_3N_4.

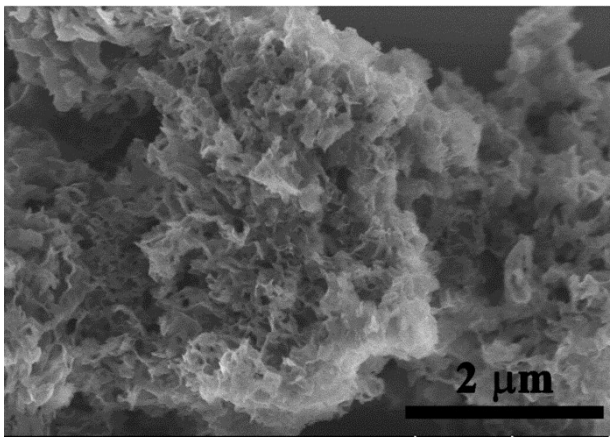

Figure S2. SEM image of CN-$UC_{0.02}$.

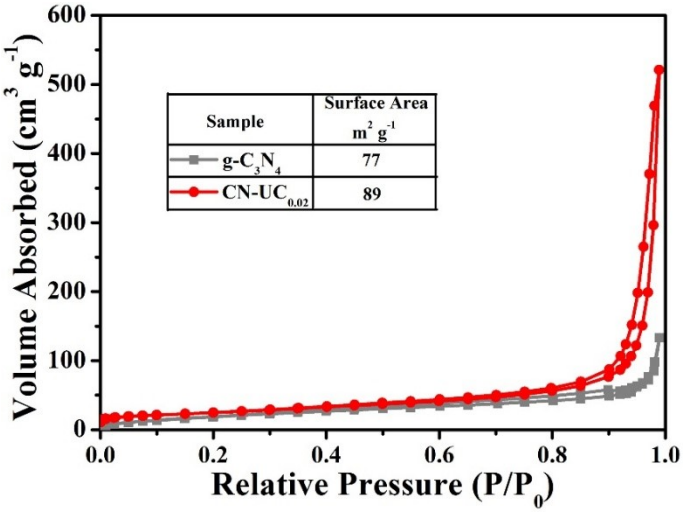

Figure S3. The BET of CN-$UC_{0.02}$ and g-C_3N_4.

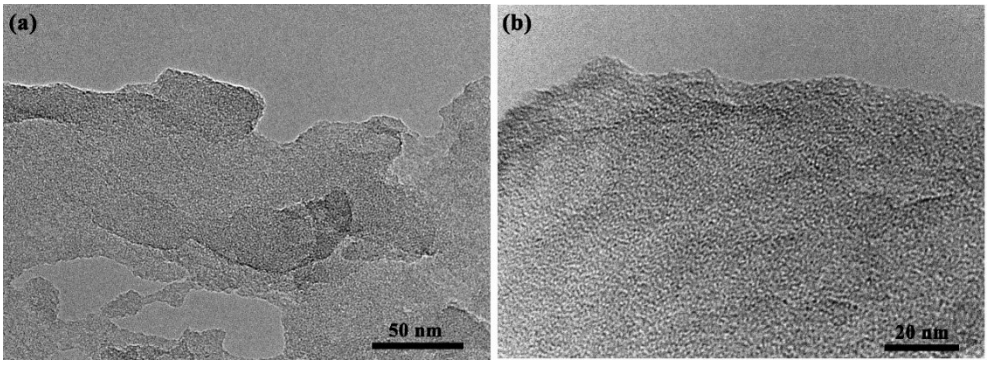

Figure S4. (a) TEM and (b) HRTEM images of g-C_3N_4.

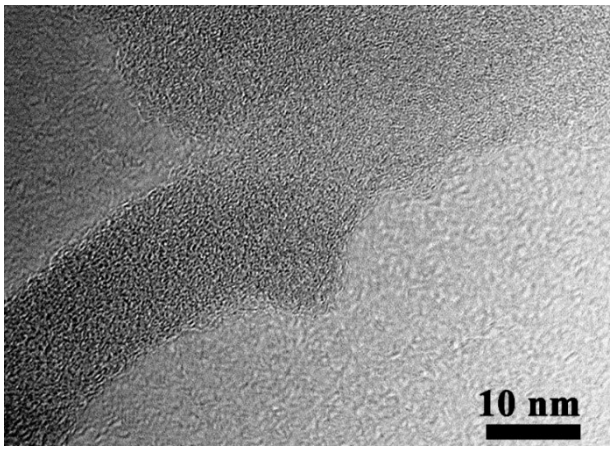

Figure S5. TEM image of CN-$UC_{0.02}$.

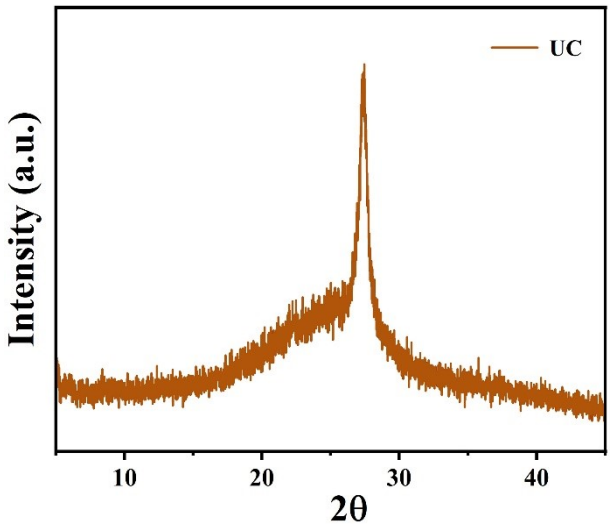

Figure R6. XRD pattern of the UC monomer.

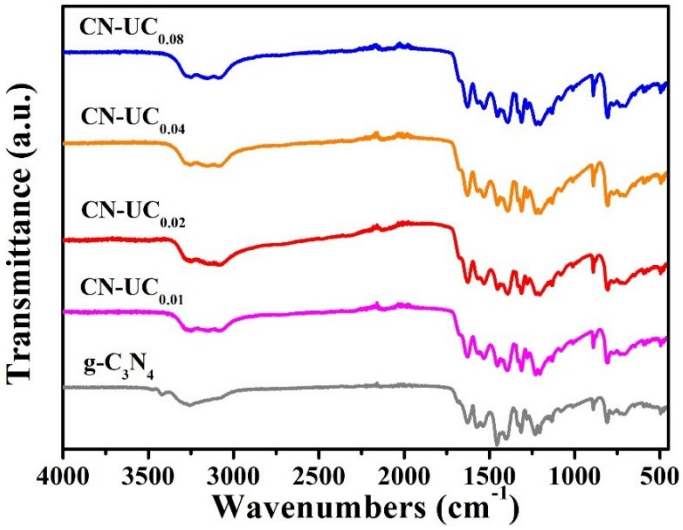

Figure S7. The FTIR spectra of different samples.

Table S1. Elemental analysis results and C/ N atomic ratio of CN-UC_x.

Sample	C / wt%	N / wt%	C/N
g-C_3N_4	34.1	61.7	0.645
CN-$UC_{0.02}$	35.4	62.1	0.665
CN-$UC_{0.04}$	35.5	60.7	0.682

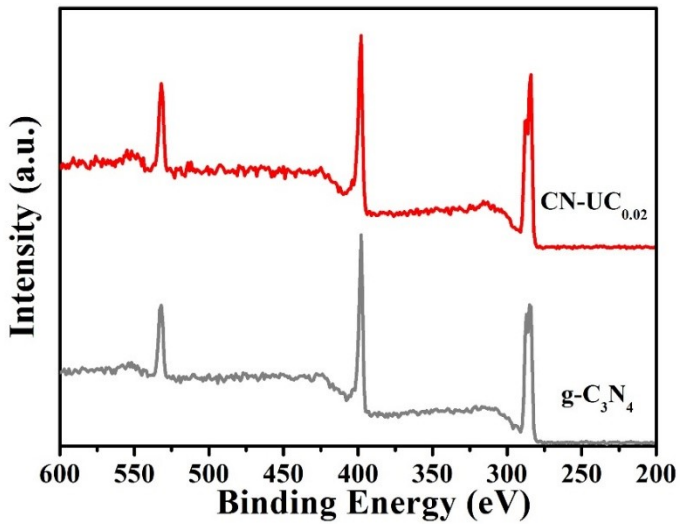

Figure S8. The full XPS of g-C_3N_4 and CN-$UC_{0.02}$.

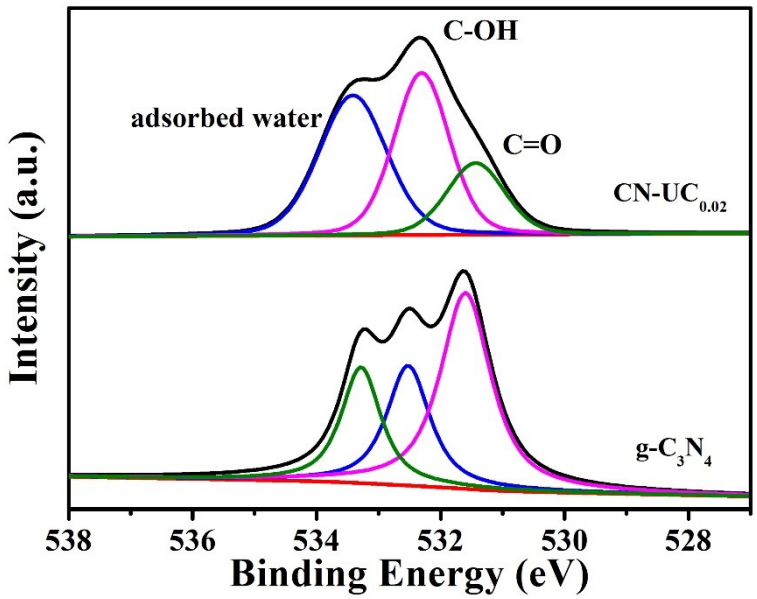

Figure S9. The O 1s XPS of g-C_3N_4 and CN-$UC_{0.02}$.

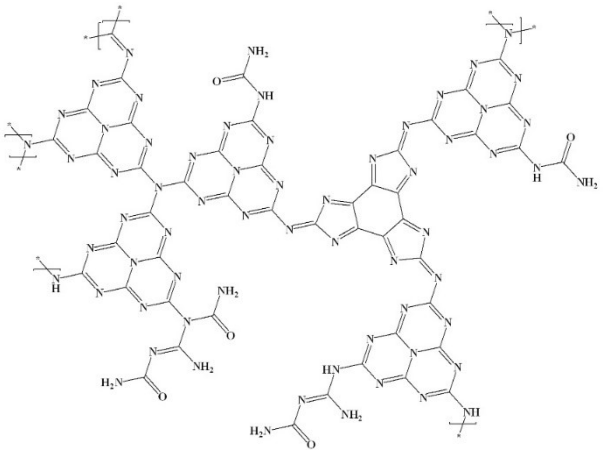

Figure S10. The proposed structure for CN-$UC_{0.02}$.

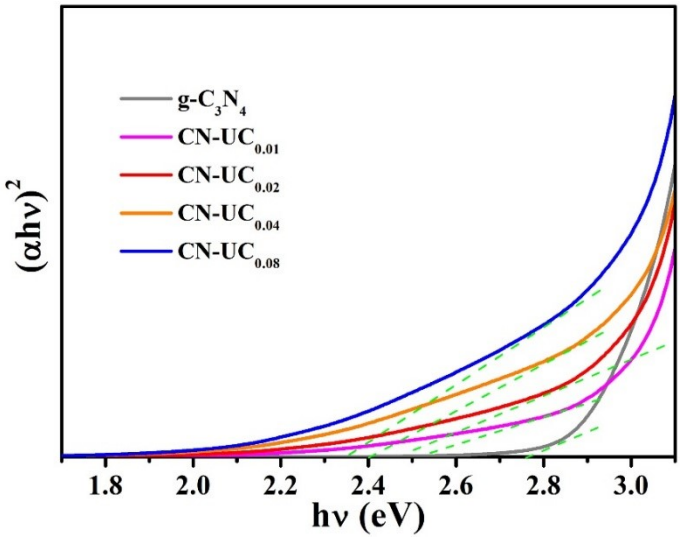

Figure S11. The band gaps of different samples.

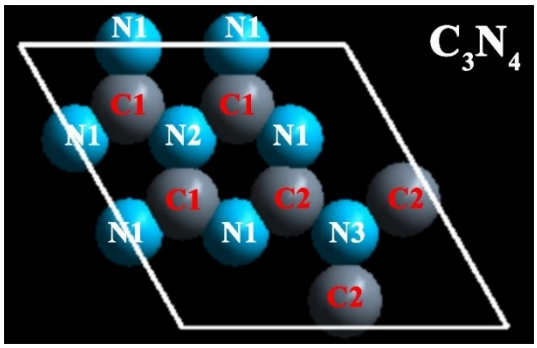

Figure S12. The theoretical calculations Model of g-C_3N_4.

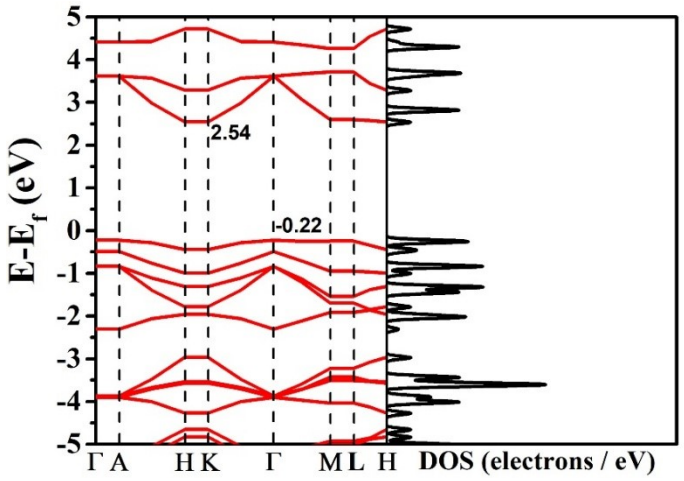

Figure S13. The DOS of g-C_3N_4.

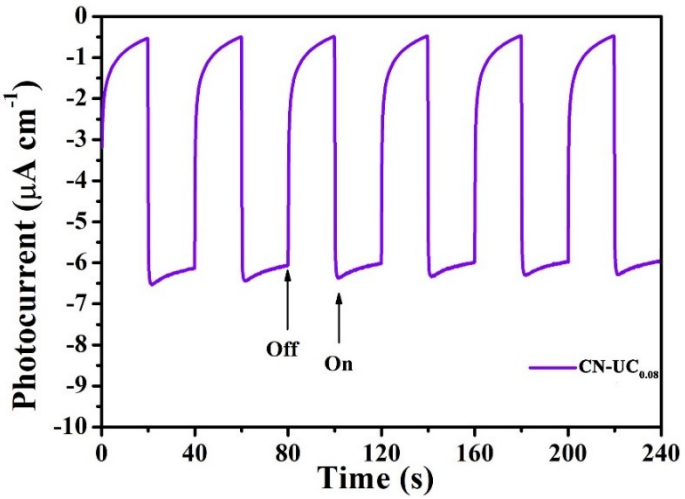

Figure S14. The transient photocurrent of CN-$UC_{0.08}$ under visible light ($\lambda \geq 420$ nm).

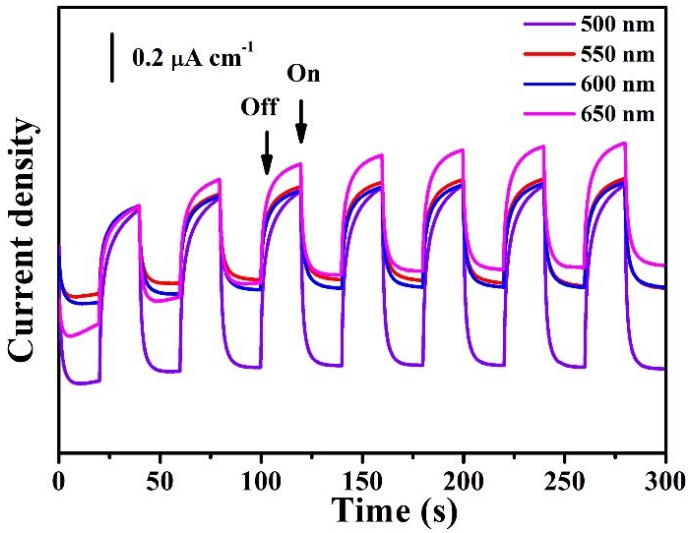

Figure S15. The transient photocurrents under different monochromatic light of CN-$UC_{0.02}$.

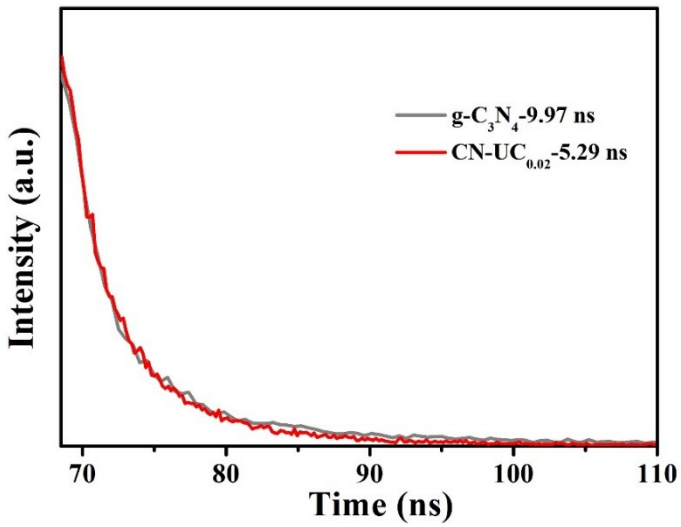

Figure S16. The fluorescence lifetime of g-C_3N_4 and CN-$UC_{0.02}$.

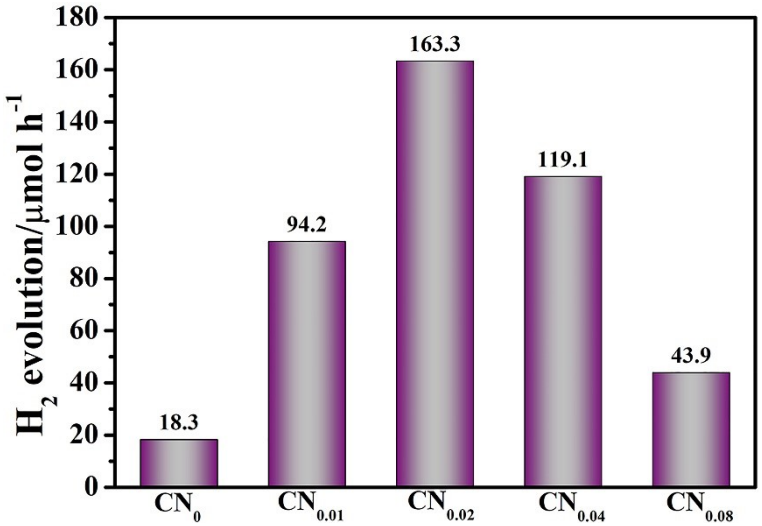

Figure S17. The Photocatalytic hydrogen evolution of different samples (10 mg).

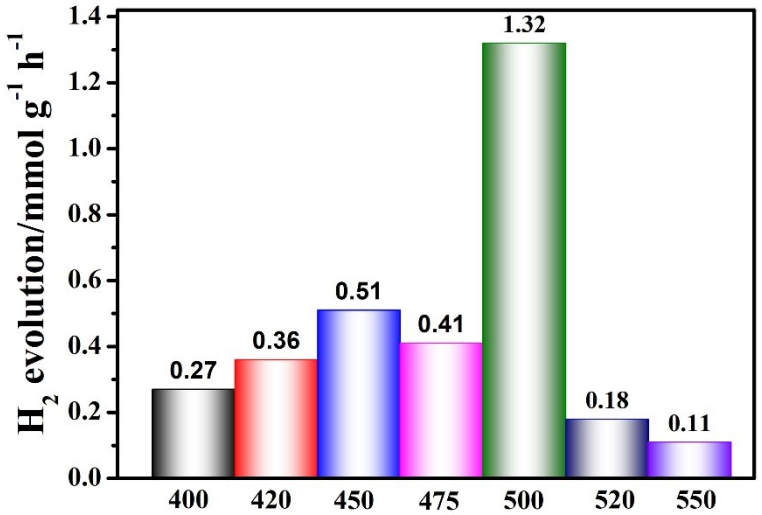

Figure S18. The hydrogen evolution of CN-$UC_{0.02}$ at different wavelengths.

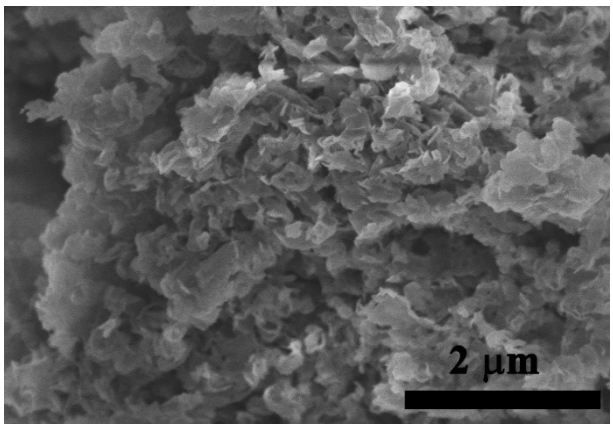

Figure S19. The SEM image of CN-$UC_{0.02}$ after reaction.

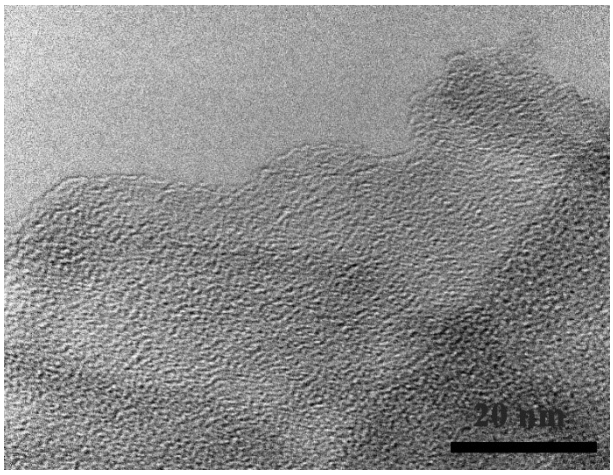

Figure S20. The TEM image of CN-$UC_{0.02}$ after reaction.

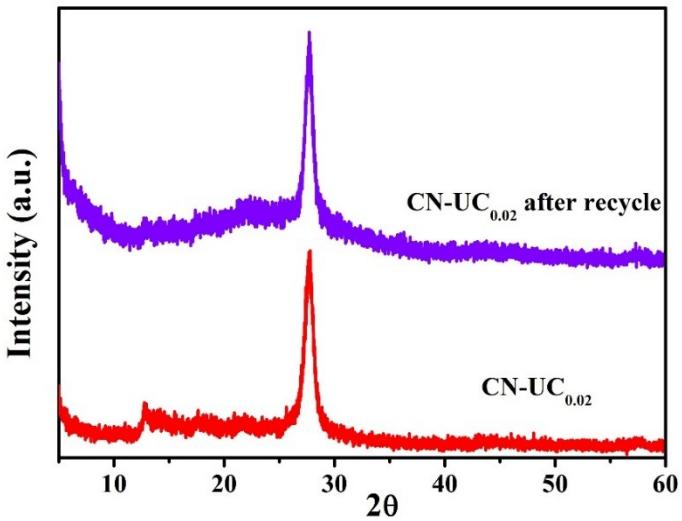

Figure S21. The XRD of CN-$UC_{0.02}$ after reaction.

Reference

[1] Y. O. Wang, F. Silveri, M. K. Bayazit, Q. S. Ruan, Y. M. Li, J. J. Xie, C. R. A. Catlow and J. W. Tang, *Adv. Energy Mater*. **2018**, 1801084.

[2] G. G. Zhang, G. S. Li, Z. A. Lan, L. H. Lin, A. Savateev, T. Heil, S. Zafeiratos, X. C. Wang and M. Antonietti, *Angew. Chem. Int. Ed*., **2017**, *56*, 13445 –13449.

[3] N. Tian, Y. H. Zhang, X. W. Li, K. Xiao, X. Du, F. Dong, G. I.N. Waterhoused, T. R. Zhang and H. W. Huang, *Nano Energy*, **2017**, *38*, 72–81.

[4] Q. Han, B. Wang, J. Gao and L. T. Qu, *Angew. Chem. Int. Ed*., **2016**, *55*, 10849 – 10853.

[5] X. J. Chen, R. Shi, Q. Chen, Z. J. Zhang, W. J. Jiang, Y. F. Zhu and T. R. Zhang, *Nano Energy*, **2019**, *59*, 644–650.

[6] X. G. Li , W. T. Bi , L. Zhang , S. Tao , W. S. Chu, Q. Zhang , Y. Luo, C. Z. Wu and Y. Xie, *Adv. Mater*.,. **2016**, *28*, 2427–2431.

[7] J. R. Ran, W. W. Guo, H. L. Wang, B. C. Zhu, J. G. Yu and S. Z. Qiao, *Adv. Mater*.,. **2018**, *30*, 1800128.